Electromagnetic and Thermal Coupled Analysis of Ferrite Orthogonal-Core Based on Three-Dimensional Reluctance and Thermal-Resistance Network Model

Kenji Nakamura, *Member, IEEE*, Hirokazu Yoshida, and Osamu Ichinokura, *Member, IEEE*

***Abstract*—In this paper, we propose an electromagnetic and thermal coupled analysis of a ferrite orthogonal-core variable inductor based on the equivalent circuit theory. A three-dimensional reluctance network model and thermal-resistance network model are combined with each other, and calculated simultaneously on a general purpose circuit simulator SPICE.**

***Index Terms*—Coupled analysis, iron loss, orthogonal-core, reluctance network analysis (RNA), SPICE, thermal-resistance network analysis, variable inductor.**

I. Introduction

An orthogonal-core has desirable features such as a simple construction and high reliability. Because of a magnetic interaction, a net inductance of secondary winding can be controlled by a primary dc current. Namely, the orthogonal-core operates as a variable inductor [1], [2].

In the electric power system, some apparatuses utilizing the variable inductor have been reported [3]–[5]. Especially, as for a VAR compensator, a trial 100-kVA apparatus for 6.6-kV distribution system has been developed, and useful results were obtained from field tests.

In recent years, the orthogonal-core variable inductor has been applied to soft switching power supplies as a tuning inductance. An optimum design method of the variable inductor for high-frequency applications is not clarified fully, and therefore needed.

We previously proposed a Reluctance Network Analysis (RNA), and applied it to an analysis of silicon steel orthogonal-core for the commercial frequency applications [5], [6]. In the high-frequency application, however, we must evaluate a core temperature rise due to an iron loss. In this paper, we propose an electromagnetic and thermal coupled analysis of a ferrite orthogonal-core variable inductor based on the equivalent circuit theory.

II. Three-Dimensional Magnetic Circuit

Fig. 1 shows the structure and windings arrangement of the orthogonal-core used for the examinations. The core material is Mn–Zn ferrite (NEC-TOKIN: BH2). Fig. 2 shows a fundamental magnetic circuit of the orthogonal-core. In the figure, we express the relationship between a magnetomotive force and flux on a reluctance as $F = k\phi^3$. The secondary magnetomotive force (MMF) is given by

$$N_2 i_2 = \left\{(3k/4)\phi_1^2 + (k/4)\phi_2^2\right\}\phi_2 \tag{1}$$

where the coefficient is k [3]. From (1), we find the secondary current is controlled by the primary excitation.

Fig. 3 shows a basic circuit of the orthogonal-core variable inductor.

For an analysis of the orthogonal-core variable inductor, a three-dimensional nonlinear magnetic field analysis is needed. We apply the RNA to the analysis of orthogonal-core. That is, we divide the orthogonal-core into some elements as shown in Fig. 4(a). In order to consider the leakage fluxes, the surrounding space is also divided. The divided elements can be expressed by a unit magnetic circuit as shown in Fig. 4(b). In the core region, characteristics of reluctance and inductance are given by

$$f_m = \left(\frac{\alpha_1 l}{S} + \frac{\alpha_n L}{S^n}\phi^{n-1}\right)\phi + \left\{\frac{\beta_1 l}{S} + \frac{\beta_m l}{S^m}\left(\frac{d\phi}{dt}\right)^{m-1}\right\}\frac{d\phi}{dt} \tag{2}$$

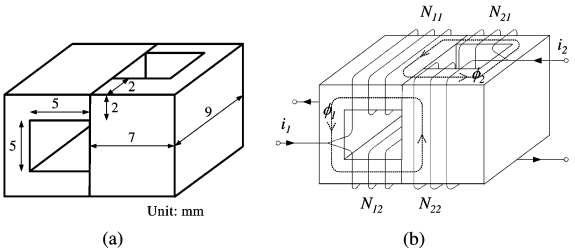

Fig. 1. Ferrite orthogonal-core used for the examinations. (a) Structure and dimensions. (b) Windings arrangement.

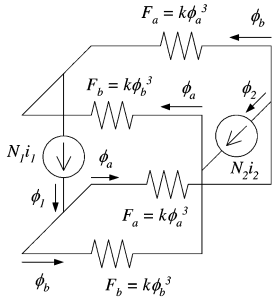

Fig. 2. Fundamental magnetic circuit of the orthogonal-core.

Manuscript received October 12, 2003.

The authors are with the Graduate School of Engineering, Tohoku University, Sendai 980-8579, Japan (e-mail: nakaken@ecei.tohoku.ac.jp; hiro@power.ecei.tohoku.ac.jp; ichinoku@ecei.tohoku.ac.jp).

Digital Object Identifier 10.1109/TMAG.2004.832497

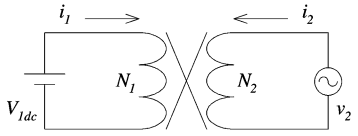

Fig. 3. Circuit configuration of the orthogonal-core variable inductor.

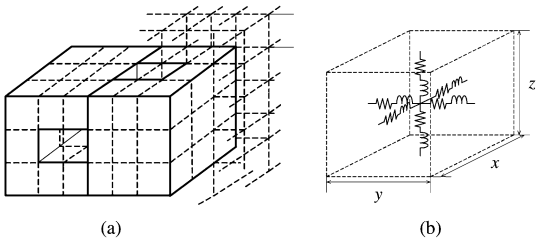

Fig. 4. Three-dimensional magnetic circuit model of the orthogonal-core based on the RNA. (a) Subdivision of the core. (b) Unit magnetic circuit.

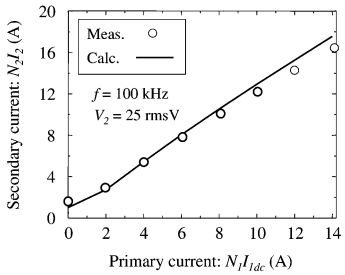

Fig. 5. Control characteristics of the orthogonal-core variable inductor.

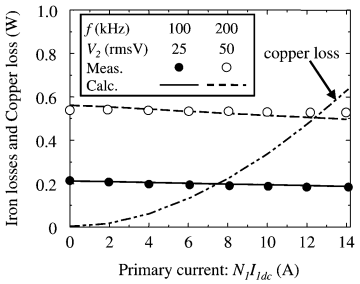

Fig. 6. Copper and iron loss characteristics of the variable inductor.

where coefficients are α_1 and $\alpha_{\rm n}$, which are determined by a B–H curve of core material. An iron loss characteristic gives the coefficients β_1 and $\beta_{\rm m}$ [6], [7]. The coefficients using the analysis are $\alpha_1 = 2.40 \times 102$ A/mT, $\alpha_{19} = 1.445 \times 10^8$ A/mT^{19}, $\beta_1 = 6.079 \times 10^{-5}$ As/mT, and $\beta_3 = 2.464 \times 10^{-16}$ As^3/mT^3, respectively. On the other hand, reluctances are determined by a permeability of free space μ_0 in the surrounding space.

The magnetic circuit model of the orthogonal-core is combined with an electric circuit by a proper method [4]. We calculate the characteristics of the orthogonal-core variable inductor on a general purpose circuit simulator SPICE.

Fig. 5 shows the control characteristics of orthogonal-core variable inductor. In the figure, the line is a calculated result; the symbols are measured values. Fig. 6 shows the iron loss characteristics. In the model, the iron loss is obtained from the stored energy of inductance shown in Fig. 4(b). From the figures, it reveals that the calculated values agree well with the experimental ones.

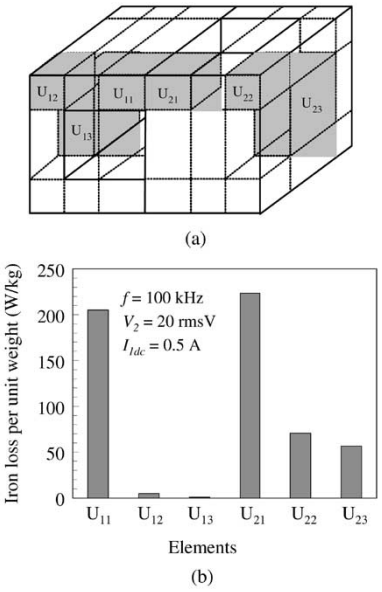

Fig. 7. Distribution of the iron loss in the orthogonal-core. (a) Selected elements. (b) Iron loss per unit weight of the selected elements.

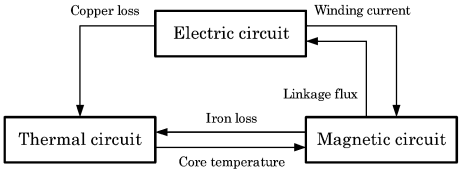

Fig. 8. Schematic diagram of the electromagnetic and thermal coupled analysis method examined in the paper.

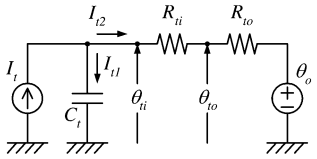

Fig. 9. Fundamental thermal equivalent circuit.

The proposed method can calculate a distribution of the iron loss in the core. Fig. 7(b) indicates the iron loss per unit weight of selected elements shown in Fig. 7(a).

III. Electromagnetic and Thermal Coupled Analysis

Fig. 8 shows the schematic diagram of the electromagnetic and thermal coupled analysis method examined in the paper. We utilize the equivalent circuit theory for the coupled analysis, and calculated on the general purpose circuit simulator SPICE.

Fig. 9 shows a basic thermal-resistance circuit model considering a radiation from a surface of an object. In the figure, a heat flow and a heat capacity are I_t and C_t, respectively. A thermal resistance and a radiation resistance are R_{ti} and R_{to}, respectively. The temperatures of an internal and surface of an object are θ_{ti} and θ_{to}, and an external space temperature is θ_o.

A thermal resistance is given by

$$R_{ti} = \frac{l_t}{\kappa S_t} \tag{3}$$

where the thermal conductivity is κ, a heat transfer path and a cross section are l_t and S_t, respectively.

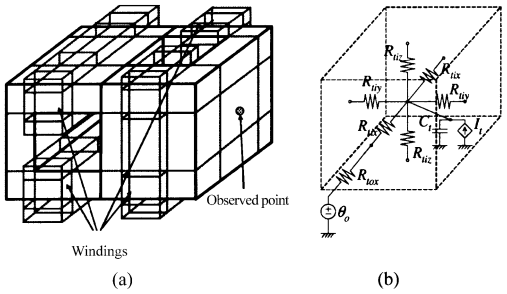

Fig. 10. Three-dimensional thermal-resistance network model and thermal observed point of secondary side (primary side is same position of primary core). (a) Subdivision of the core and windings. (b) Unit thermal-resistance circuit.

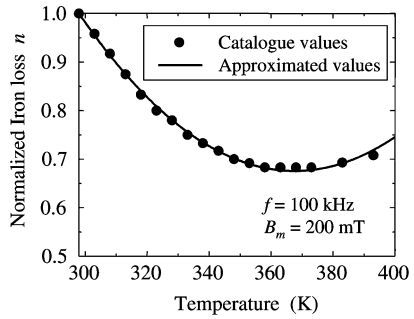

Fig. 11. Relationship between the iron loss and the core temperature.

A radiation resistance is expressed as follows:

$$R_{to} = \frac{\theta_{to} - \theta_o}{I_o} = \frac{1}{(h_c + h_r)A} \tag{4}$$

where a heat flow to an external space is I_o. A convection heat transfer coefficient and a radiation heat transfer coefficient are h_c and h_r, respectively. These are given by

$$h_c = 2.51 \times 1.39 \times \left(\frac{\theta_{to} - \theta_o}{L}\right)^{0.25} \tag{5}$$

$$h_r = \frac{5.67 \times 10^{-8} \varepsilon \left\{\theta_{to}^4 - \theta_o^4\right\}}{\theta_{\rm to} - \theta_o}. \tag{6}$$

In the (5), a length of an object is L. The coefficients are 2.51 and 1.39, which depend on a fluid type of external space, structure of object, and a state of installation. Therefore, the coefficients are derived semi-empirically from the theory and experimental values. In the (6), Stefan-Boltzmann's coefficient is 5.67×10^{-8}, and an emissivity of an object is ε.

Based on the above mentioned, a thermal-resistance network model of the orthogonal-core is constructed. The method of the construction is similar to the reluctance network model. That is, the orthogonal-core including the windings is divided into some elements as shown in Fig. 10(a). The divided elements are replaced by a unit thermal-resistance circuit. In the unit circuit, resistances are given by the (3). The heat flow source is connected to the unit circuit. In the winding region, the heat flow is given by a copper loss. In the core region, given by an iron loss. Furthermore, since an iron loss of a ferrite core depends on a core temperature as shown in Fig. 11, we consider the influence for the analysis by representing the coefficients β_1 and β_m as a function of temperature.

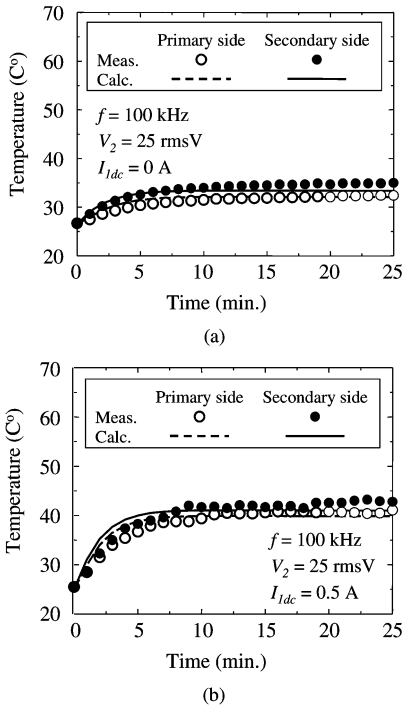

Fig. 12. Core temperature transient characteristics. (a) $f = 100$ kHz, $I_{1\rm dc} = 0$ A. (b) $f = 100$ kHz, $I_{1\rm dc} = 0.5$ A.

Fig. 12 shows the core temperature transient characteristics of the orthogonal-core variable inductor. Lines are calculation results obtained by the coupled analysis, and symbols are experimental ones. It reveals that the calculated values agree well with the experimental ones.

IV. Conclusion

We proposed the electromagnetic and thermal coupled analysis of the ferrite orthogonal-core variable inductor based on the equivalent circuit theory. Using the proposed method, we can calculate simultaneously the winding currents, copper and iron losses, and core temperature. The proposed method is useful for the optimum design of ferrite orthogonal-core in a high-frequency region.

References

[1] S. D. Wanlass, "The paraformer," in *IEEE Wescon Tech. Papers*, vol. 12, 1968.

[2] O. Ichinokura, S. Kikuchi, and K. Murakami, "A new ac power stabilizer using two-orthogonal-core type parametric transformer and variable inductor," *IEEE Trans. Magn.*, vol. MAG-18, pp. 1761–1763, 1982.

[3] O. Ichinokura, T. Jinzenji, and K. Tajima, "A new variable inductor for VAR compensation," *IEEE Trans. Magn.*, vol. 29, pp. 3225–3227, Nov. 1993.

[4] K. Nakamura, O. Ichinokura, M. Kawakami, M. Maeda, S. Akatsuka, K. Takasugi, and H. Sato, "Analysis of orthogonal-core type linear variable inductor and application to VAR compensator," *IEEE Trans. Magn.*, vol. 36, pp. 3565–3567, Sept. 2000.

[5] K. Nakamura, O. Ichinokura, M. Kawakami, M. Maeda, and H. Sato, "Application of orthogonal-core transformer to series compensation for power system," *IEEE Trans. Magn.*, vol. 37, pp. 2858–2861, July 2001.

[6] K. Tajima, A. Kaga, Y. Anazawa, and O. Ichinokura, "One method for calculating flux-MMF relationship of orthogonal-core," *IEEE Trans. Magn.*, vol. 29, pp. 3219–3221, Nov. 1993.

[7] K. Tajima, Y. Anazawa, T. Komukai, and O. Ichinokura, "An analytical method for characteristics of orthogonal-core under consideration of magnetic saturation and hysteresis," in *Proc. EPE'97*, 1997, pp. 2.006–2.011.